Predicting wake meandering in real-time through instantaneous measurements of wind turbine load fluctuations

S Aubrun[1], YA Muller[1,2], C Masson[2]

[1] Univ. Orléans, INSA-CVL, PRISME EA-4229, 8, rue Léonard deVinci, 45072 Orléans Cedex 2, France

[2]Ecole de Technologie Supérieure, 1100, rue Notre‑Dame Ouest, Montréal H3C 1K3, Canada

E-mail: sandrine.aubrun@univ-orleans.fr

Abstract. The present study deals with the real-time estimation of the wind turbine wake meandering and the determination of the best indicators to measure in order to build a real-time wake meandering model. Results are obtained through experiments performed in an atmospheric boundary layer wind tunnel, where a specific set-up enables to measure simultaneously the incoming lateral velocity fluctuations, the lateral force fluctuations applied to the wind turbine model and to track in real-time the lateral position of its wake. It is an extension of a previous work about the determination of good candidates to build some real-time predictors of the wake meandering. The strong correlations between the incoming transverse velocity fluctuations, the lateral force fluctuations and the lateral position of the wake farther downstream are quantified, confirming that the large-scale turbulent eddies impact directly the wake meandering. Three different versions of a wake meandering predictor model are compared. It leads to the conclusion that the monitoring of the global force fluctuations applied to a wind turbine could be used to predict in real-time the meandering of the generated wake.

1. Introduction

Wind turbine wake interactions are one source of power losses in wind farms. Their predictions are inaccurate since the wake models implemented in commercial wind resource assessment models are very basic. For instance, they do not take into account the atmospheric flow conditions and its unsteady features [1-3]. However, the large scale turbulent eddies contained in the atmospheric boundary layer (ABL) represent one source of the meandering process of the wind turbine wake, which is characterized mainly by low frequency horizontal oscillations of the whole wake [4-6]. The present study is exclusively focused on this source of meandering. Some meandering wake models were developed based on this hypothesis [7-9]. PRISME Laboratory from the University of Orléans already performed several experiments in its atmospheric boundary layer test section of the Malavard wind tunnel in order to prove the existence of this phenomenon and characterize it [10-12]. It had already obtained a transfer function between the incoming flow turbulent properties and the wake meandering, giving the possibility to predict in real-time the main meandering behavior of the wake just by monitoring the incoming flow [13]. This result could be used in numerical models of meandering but one could also think of applying this procedure in real time and in real-configurations in order to improve the wind farm monitoring and control. On the other hand, it is not yet common to have access to the measurements

of the incoming flow of a wind turbine (even if the LIDAR technology is mature enough to enable the development of LIDAR-assisted control systems [14]) and our goal in this present work is to determine a better candidate than the incoming flow velocity as meandering predictor.

It is expected that the global unsteady aerodynamic loads applied to the wind turbine could be adapted to this application and an experiment had been designed on in order to prove this expectation.

The results showed that the global drift force fluctuations measured on the actuator disc, which are a signature of the integrated transverse velocity fluctuations all over the disc and can be interpreted as an unsteady misalignment of the rotor according to the incoming flow, are also correlated with the meandering process. A correlation between the vertical torque (yaw) fluctuations and the meandering is identified when the modeled wind turbine interacts with an upstream wind turbine wake. It was concluded that the yaw fluctuations could be a good indicator of the presence of an upstream wake [13]. The present work will be dedicated to combine these results with a model dealing with the horizontal wake deviation versus the misalignment angle in order to determine whether this unsteady misalignment can be a source of amplification of the meandering.

2. Experimental set-up

The present experiments are based on the physical modelling in a wind tunnel of the ABL and of the wind turbine at a very reduced geometric scale (1:400). This ABL modelling approach is extensively used in atmospheric dispersion applications for 50 years and more recently in wind energy applications. Several referenced guidelines and articles described precisely the rules to properly reproduce an ABL in a wind tunnel and the limitations of this modelling [15-19]. For instance, the fact that the characteristic Reynolds number of the model is much smaller than in full scale must be particularly studied. Even if a critical Reynolds number based on the obstacle dimensions of 10,000 had been established to ensure the Reynolds independency of obtained results, this independency must be checked by reproducing experiments at different reference velocities. Additionally, any element composing the model must be smooth in order to avoid the re-laminarization process. These constraints were taken into account in the present set-up. The strategy to model the wind turbine was also driven by these constraints: the rotor is modelled by a porous disc made of metallic mesh. The flow through a porous grid (i.e. a turbulence grid) is known to be Reynolds independent [20]. Additionally, this modelling concept eliminates the unsteady flow signatures due to the blade motion (blade wake, rotational momentum, tip vortex, root vortex) and due to the massive separation (Van Karman-type vortices as in a bluff-body wake). It therefore ensures that, if a meandering process is detected, it is only due to the interactions between the incoming turbulent length scales and the wind turbine [11, 12]. The remaining discrepancies related to the relatively low Reynolds number is the modification of the dissipation scales but they do not play a role in the present scenario of meandering process, based on the large turbulent scales.

The experiments were carried out in the "Lucien Malavard" wind tunnel located at the PRISME Laboratory from the University of Orléans (Fig. 1). The wind tunnel is equipped to model a neutrally stratified ABL flow at a geometric scale of 1:400. In order to obtain a model of a moderately rough ABL, the 14m development plate is covered with perforated steel sheet. Furthermore a turbulence grid, combined with turbulence generators, is located at the entrance of the wind tunnel section in order to initiate appropriate mean velocity and turbulence intensity profiles. Although the return test section is 4m×4m, the effective test area is 3m wide and 1.5m high.

Properties of the obtained boundary layer (mean velocity, turbulence intensity and integral length scale profiles) are checked and are in agreement with the standards for ABL flows [15-19]. The ABL is representative of a moderately rough terrain, with a roughness length of $z_0 = 5.10^{-5}$m (equivalent full scale roughness length of 0.02m), a power law exponent of $\alpha = 0.14$ and a friction velocity of $u^* = 0.29$m.s^{-1}. The mean velocity measured at hub height is $U_\infty = 6.9$ m.s^{-1}. The turbulence intensity profiles are within the expected range for this type of terrain and the expected ratio between the turbulence intensities $Iw/Iu = 0.5$ is obtained. The streamwise integral length scale Lu_x is relatively constant at the height of interest and is 2 to 4 times larger than the rotor diameter. This ensures that the meandering process due to the presence of large turbulent eddies in the incoming flow can exist.

The modelling concept of the wind turbine is based on the actuator disc theory as described by Aubrun et al [10]. The rotor is reproduced with a disc of metallic mesh of 200mm of diameter (***D***) (80m at full scale). The solidity of the porous disc is 45% (wire diameter of 1mm and thread spacing of 3.2mm), leading to an equivalent axial induction factor of $a = 0.19$ (defined in §3.2) and a thrust coefficient of $C_T = 0.62$. The center of the porous disc is located at a variable hub height H_{hub} with a threaded rod with a $0.05D$ diameter.

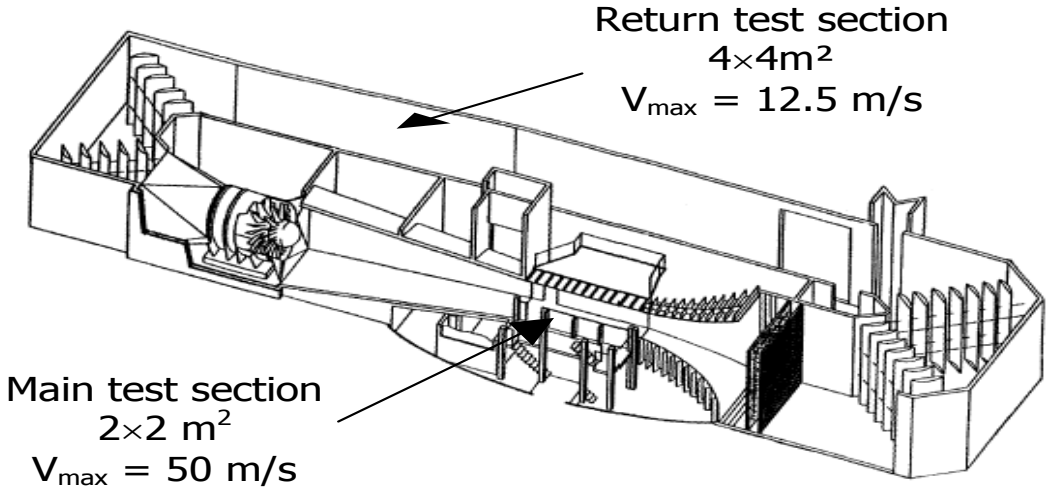

Figure 1. The "Lucien Malavard" wind tunnel of PRISME Laboratory, University of Orléans. Measurements were performed in the return test circuit, adapted to model a neutrally stratified atmospheric boundary layer

A horizontal hot wire rake composed of 5 hot wire probes (four 55P11 single probes, one 55P61 X-probe and anemometers from Dantec Dynamics) located at a distance $L=5D$ downstream of the wind turbine is used to determine the instantaneous horizontal wake position (Fig. 2).

The choice is made to focus the whole study only on the horizontal meandering since it has been observed that it is the main meandering direction due to the fact that the horizontal turbulent velocity fluctuations in a turbulent boundary layer are larger than the vertical ones, which is itself a consequence of the blockage effect by the ground [11, 18].

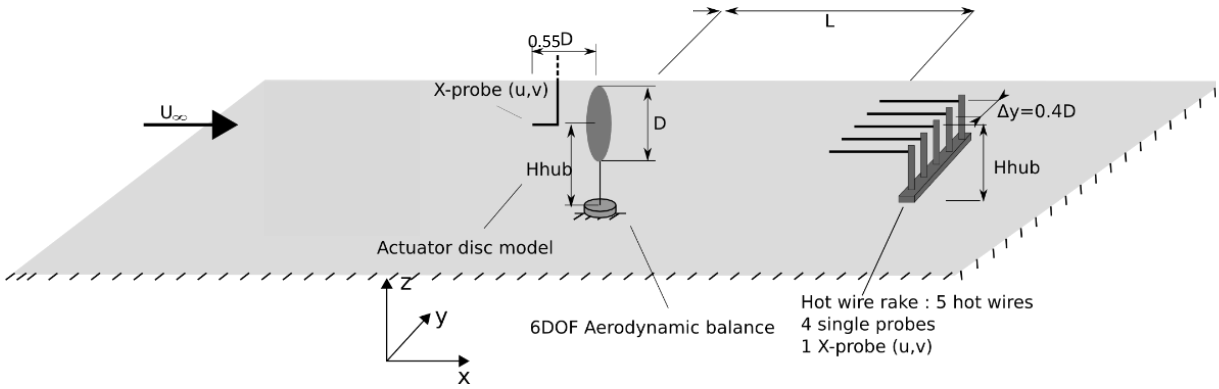

Figure 2. Experimental set-up and dimensions.

On one side of the rake, the X hot-wire probe is used in order to measure the local transverse velocity fluctuations. The uniform spacing between probes is $\Delta y = 0.4D$. The methodology to calculate the horizontal wake position is based on the computation of a weighted average of the locations of each

probe (which are fixed), where the weighting is chosen as the exponential of the instantaneous local velocity deficit (see details and validation in [13]).

A 55P61 DANTEC hot wire X-probe is located 0.55D upstream of the wind turbine model of interest, measuring the horizontal components of the velocity.

The wind turbine model is fixed on a 6-axis aerodynamic balance (ATI Mini40), which is located underneath the floor. The three components of the aerodynamic force (F_x, F_y, F_z) and the three components of the associated torque (T_x, T_y, T_z) computed according to the center of the rotor model are measured. The 6 channels of the aerodynamic balance are simultaneously acquired with the hot wire time series so as to allow time correlations.

3. Results and discussion

3.1. Coherence and phase shift

In order to assess the relationship between the upstream large scale turbulence, the global load fluctuations and wake meandering, the coherences and the associated phase shifts are computed between the upstream transverse velocity $v_{upstream}$, the lateral force F_y and the wake position y_w (Fig. 3). The coherence is defined as a dimensionless value deduced from the cross-spectrum and in the range between 0 (no correlation) and 1 (full correlation), as a function of the frequency.

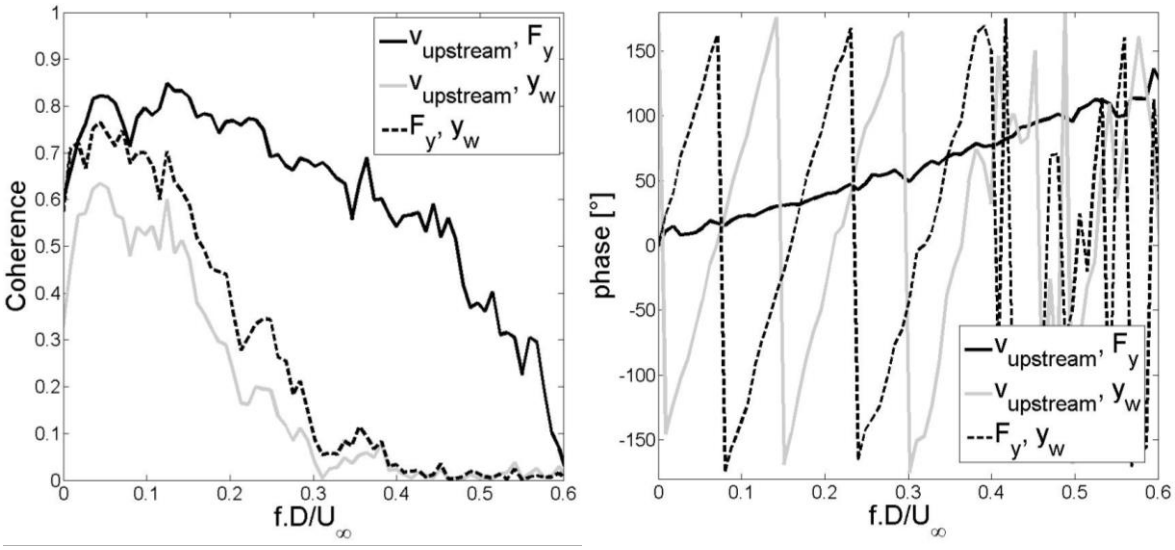

Figure 3. Coherence and phase shift between physical values.

The coherence between the upstream transverse velocity $v_{upstream}$ and the lateral force F_y shows a very high level of coherence over a broad frequency range and reaches the value of 0.8 for low frequencies. The associated phase shift presents a linear law versus the frequency that is representative of a convective phenomenon. The slope of the linear law is directly linked to the time delay between both signals. It is assessed to $\tau_{F/v}$= 16.4 ms, which leads to a convection velocity $Uc_{F/v}$=0.55 $\boldsymbol{D}/\tau_{F/v}$ = 0.98$\boldsymbol{U}_\infty$. It illustrates that the lateral load fluctuations measured on the wind turbine model are directly driven by the incoming transverse velocity fluctuations, with a time delay due to the streamwise advection.

The coherence between the upstream transverse velocity $v_{upstream}$ and the lateral wake position y_w shows a lower level of coherence since it reaches only a value of 0.6 and the frequency range of correlation is also narrower. Indeed, the coherence tends to zero for $f.D/U_\infty$ = 0.3. One can associate this cut-off frequency to length scales of 0.33$\boldsymbol{D}$, leading to the conclusion that only the turbulent eddies larger than 0.33$\boldsymbol{D}$ contribute to the wake meandering signature that is captured in the present experiment.

On the other hand, previous results showed that the spectral content of the meandering process was assessed to be significant up to $f.D/U_\infty = 0.5$ [13]. The long distance between both signals $\boldsymbol{L}$+0.55$\boldsymbol{D}$ = 5.55$\boldsymbol{D}$, which is higher than 2 times $\boldsymbol{Lu_x}$ is the reason of the correlation loss for the intermediary turbulent eddies. They are more rapidly distorted and renewed than the larger ones during the advection process.

The associated phase shift between upstream transverse velocity $v_{upstream}$ and the lateral wake position y_w presents also a linear law versus the frequency. The time delay between signal is assessed to $\tau_{v/y}$= 202.2 ms, which leads to a convection velocity $Uc_{v/y}$=5.55 $\boldsymbol{D}/\tau_{v/y}$ = 0.8$\boldsymbol{U}_\infty \approx$ (1-$\boldsymbol{a}$) $\boldsymbol{U}_\infty$. This information confirms that the meandering process, illustrated here by the lateral wake position fluctuations y_w, is mainly driven by the transverse velocity fluctuations that impact the wind turbine model.

The coherence between the lateral force F_y and the lateral wake position y_w, the associated phase shift and convection velocity $\tau_{F/y}$ are similar as the previous one. The maximum level of coherence is slightly higher with 0.7 instead of 0.6. This information is of interest since lateral force fluctuations are an image of the interactions between the yawed flow and the actuator disc. Having a higher coherence level between the position of the wake and the force than between the wake and the velocity tends to indicate that theses interactions should not be neglected into the wake meandering models.

3.2. Unsteady yaw effects.

The presence of transverse velocity fluctuations can be considered as an unsteady yaw effect, where $\gamma(t)$ is the angle between the instantaneous horizontal velocity vector and the streamwise direction. This instantaneous yaw angle is assessed with the following equation:

$$\gamma(t) = tan^{-1}\left(\frac{v_{upstream(t)}}{U_\infty}\right) \quad (1)$$

According to the vortex cylinder theory of a yawed actuator disc [21], the induced velocity that actually impacts the disc is skewed from an angle χ, with χ the skew angle of the wake, which is related to the axial induction factor a and the yaw angle γ:

$$\chi = (0.6a + 1)\gamma \quad (2)$$

With $a = 1 - \frac{U_{disc}}{U_\infty} = \frac{1}{2}\left(1 - \frac{U_{wake}}{U_\infty}\right)$, U_{disc} is the streamwise velocity at the disc location and U_{wake} is the streamwise velocity in the far-wake.

This formula is demonstrated for a steady yaw but it is attempted to extrapolate it to the present unsteady analysis, considering that a hypothesis of quasi-steadiness (succession of steady states) is acceptable for yaw modifications at low frequency.

If one expects that the lateral force fluctuations $F_y(t)$ are directly related to the induced velocity fluctuations that impact the disc, and that the instantaneous angle between the horizontal force vector and the streamwise direction $\theta_F(t)$ is equal to the angle between the instantaneous induced velocity vector and the streamwise direction:

$$\theta_F(t) = \chi(t) = (0.6a + 1)\gamma\left(t - \tau_{\mathrm{F/v}}\right) = G_{\theta_F/\gamma\,theo}.\gamma\left(t - \tau_{\mathrm{F/v}}\right) \quad (3)$$

With $G_{\theta_F/\gamma\,theo} = 1.11$ in the present configuration.

Fig. 4 shows the gain of the transfer function between the angles $\gamma(t)$ and $\theta_F(t)$ deduced from the experiments, $G_{\theta_F/\gamma\,exp}(f)$. It is relatively constant all over the presented frequency range at a value of 0.4. Even if this is the right order of magnitude, it shows that the relationship between the unsteady yaw angle and the unsteady drift (lateral force $\boldsymbol{F_y}$) needs to be improved. One explanation might be that the

velocity probe measuring the incoming flow is to close to the disc (0.55***D***) and that the local flow is already distorted due to the whole stream tube deflection or that the force vector is not aligned with the averaged induced velocity at the disc location. This point must be checked in a future measurement campaign.

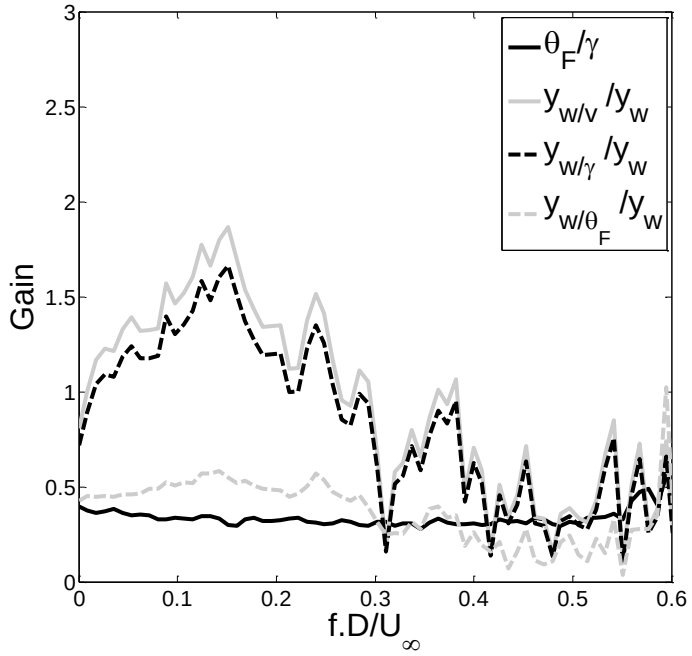

Figure 4. Gain obtained from the transfer function between physical values.
Example: $G_{Y/X}$ corresponds to the gain obtained from the transfer function estimate between the time series $X(t)$ (input) and $Y(t)$ (output)

3.3. Wake meandering models

This experimental set-up gives the opportunity to test and validate some assumptions that are used in wake meandering models as the passive transport of the wake "emitted" from the wind turbine by the incoming turbulent flow [7]. The lateral wake position at an instant t_i and at a fixed downstream distance $\boldsymbol{L}$ is expected to be totally driven by the transverse velocity fluctuations that impact the disc at the instant $(t_i - U/L)$, with U the mean streamwise velocity. In the present study, the convection velocity has been assessed to $\boldsymbol{Uc_{w/y}}$=0.8$\boldsymbol{U_\infty}$, thanks to the phase shift between the upstream transverse velocity fluctuations and the wake position fluctuations. It will be therefore used in the tested wake meandering model:

$$y_{w/v}(t) = \frac{L}{Uc_{v/y}} v_{upstream}\left(t - \tau_{v/y}\right) \tag{4}$$

In their model, the notion of passive transport of the wake is a very strong hypothesis that ignores the effects of interactions between the flow and the wind turbine model. Indeed, there is a strong coupling between the wind turbine misalignment characterized by the yaw angle and the skewed wake characterized by the skew angle. This can be taken into account into an alternative wake meandering model, considering that the meandering is directly due to the skewness of the wake:

$$\begin{aligned} y_{w/\gamma}(t) &= L.tan\left(\chi\left(t - \tau_{v/y}\right)\right) = L.tan\left((0.6a + 1)\,\gamma\left(t - \tau_{v/y}\right)\right) \\ &= L.tan\left((0.6a + 1)\,tan^{-1}\left(\frac{v_{upstream}\left(t - \tau_{v/y}\right)}{U_\infty}\right)\right) \end{aligned} \tag{5}$$

The same hypothesis of strong coupling between the flow and the actuator disc is now used to find a relationship between the lateral force fluctuations and the wake meandering, by considering that the force vector is aligned with the induced velocity at the disc location :

$$y_{w/\theta_F}(t) = L.tan\left(\chi\left(t-\tau_{F/y}\right)\right) = L.tan\left(tan^{-1}\left(\frac{F_{y\left(t-\tau_{F/y}\right)}}{\overline{F_x}}\right)\right) \quad (6)$$

Fig. 4 shows the gain of the transfer functions between the measured instantaneous lateral wake position $y_w(t)$ and the assessed ones from the three models:

- the model 1, based on the passive transport hypothesis $y_{w/v}(t)$, $G_{y_{w/v}/y_w}(f)$,
- the model 2, based on the yaw effect to the skewness of the wake $y_{w/\gamma}(t)$, $G_{y_{w/\gamma}/y_{w/}}(f)$.
- The model 3, based on the yaw effect to the skewness of the wake $y_{w/\theta_F}(t)$, $G_{y_{w/\theta_F}/y_{w/}}(f)$

If one model is correct, it is expected that its gain is close to 1 in the frequency range of interest ($f.D/U_\infty < 0.3$).

The model 1 presents a gain between 1 and 2. It means that the model proposed by Larsen et al. [7] overestimates the lateral transport of the wake. For the model 2, the gain is slightly lower than for the passive transport hypothesis but still overestimates the meandering. For the model 3, the gain is close to 0.5 for the whole frequency range of interest In that case, the meandering is overestimated. It seems that this latter model based on the measurement of the instantaneous lateral force fluctuations could also be a good candidate to predict the wake meandering since these fluctuations are very much correlated with the incoming flow fluctuations. But the gain of the transfer function is not more appropriate than the ones based on the velocity fluctuations.

4. Conclusion

The present study was performed through atmospheric boundary layer wind tunnel testing, where a specific set-up enabled to measure simultaneously the incoming lateral velocity fluctuations, the lateral force fluctuations applied to the wind turbine model and to track in real-time the lateral position of its wake. It is an extension of the work presented in [13] about the determination of good candidates to build some real-time predictors of the wake meandering. The strong correlations between the incoming transverse velocity fluctuations, the lateral force fluctuations and the lateral position of the wake farther downstream were quantified, showing that, at 5D downstream of the wind turbine model, the large-scale turbulent eddies (larger than 3***D***) impact directly the wake meandering. Three different versions of a wake meandering predictor model were compared. The first one was developed by Larsen et al. [7] and was based on the classical hypothesis of passive transport of the wake by the large turbulent eddies. The second and third ones were proposed in the present study. They were based on the hypothesis that the interactions between the incoming flow and the wind turbine model must not be neglected and took into account the skewness of the wake due to the unsteady yaw effect. The second one used as indicator the incoming velocity fluctuations, whereas the third one used the lateral force fluctuations. It was observed that none of them was able to reproduce the right magnitude of meandering. It leads to the conclusion that the monitoring of the global force fluctuations applied to a wind turbine could also be used to predict in real-time the meandering of the generated wake but the function transfer between this information and the meandering magnitude must be improved.

This study must be extended to multiple configurations through a parametrical study, in order to confirm these conclusions. The influence of the disc porosity (and so the velocity deficit and the wake skewness), the incoming wind properties (turbulence intensity and turbulence length scales) and the streamwise distance between the wind turbine model and the location where the meandering is predicted will be tested. The model sensitivity to a steady misalignment (static yaw errors encountered on real wind turbines) will be also quantified. This parametrical study might be also accompanied by LES computations.

References

[1] Ainslie JP (1988) Calculating the flow field in the wake of wind turbines, J. Wind Eng. Ind. Aerodyn. 27:213-224.
[2] Jensen NO (1983) A note on wind generator interaction. Risø Report M-2411
[3] Frandsen S, Barthelmie R, Pryor S, Rathmann O, Larsen S, Højstrup J, Thøgersen M (2006) Analytical modelling of wind Speed deficit in large offshore wind farms. Wind Energy 9:39–53
[4] Taylor GJ, Milborrow DJ, McIntosh DN, Swift-Hook DT (1985) Wake measurements on the Nibe windmills. Proceedings of the 7th British Wind Energy Association Conference March 27-29 1985, Oxford
[5] Bingöl F, Mann J and Larsen GC, (2010) Light detection and ranging measurements of wake dynamics. Part 1: one-dimensional scanning, Wind Energy 13:51–61
[6] Trujillo JJ, Bingöl F, Larsen GC, Mann J (2011) Light detection and ranging measurements on wake dynamics, Part II: Two-dimensional Scanning. Wind Energy 14:61-75
[7] Larsen G.C., Madsen H. A, Thomsen K. and Larsen T. J., (2008), Wake meandering – a pragmatic approach, Wind Energy, 11:377-395
[8] Larsen TJ, Madsen HA, Larsen GC, Hansen KS (2013) Validation of the dynamic wake meander model for loads and power production in the Egmond aan Zee wind farm. Wind Energy 16/4: 605–624
[9] Trujillo JJ, Kühn M (2009) Adaptation of a Lagrangian Dispersion Model for Wind Turbine Wake Meandering, in Proceedings of the EWEA Conference, March 16-19, Marseille, France
[10] Aubrun S, Devinant P, España G, (2007) Physical modelling of the far wake from wind turbines. Application to wind turbine interactions, Proceedings of the European Wind Energy Conference, Milan, Italy.
[11] España G, Aubrun S, Loyer S, Devinant P (2011) Spatial study of the wake meandering using modelled wind turbines in a wind tunnel. Wind Energy 14:923-937
[12] España G, Aubrun S, Loyer S, Devinant P (2012) Wind tunnel study of the wake meandering downstream of a modelled wind turbine as an effect of large scale turbulent eddies. J. Wind Eng. Ind. Aerodyn. 101:24-33
[13] Muller YA, Aubrun S, Masson C (2015) Determination of real‐time predictors of the wind turbine wake meandering, Exp Fluids DOI 10.1007/s00348-015-1923-9.
[14] Davoust S, Jehu A, Bouillet M, Bardon M, Vercherin B, Scholbrock A, Fleming P, Wright A (2014) Assessment and Optimization of LiDAR Measurement Availability for Wind Turbine Control. Scientific. Proceedings of EWEA Conference March 10-13, 2014, Barcelona, Spain
[15] Counihan J (1975) Adiabatic atmospheric boundary layers: a review and analysis of data from the period 1880-1972. Atmos. Environ. 9:871-905
[16] Snyder WH (1981) Guideline for fluid modelling of atmospheric diffusion. US Environmental Protection Agency. Report EPA-600/8-81-009
[17] Engineering Sciences Data Unit (1985) Characteristics of atmospheric turbulence near the ground. Item N° 85020
[18] Kaimal JC, Finnigan JJ (1994) Atmospheric boundary layer flows, their structure and measurements. Oxford University Press
[19] VDI guideline 3783/12 (2000) Physical modelling of flow and dispersion processes in the atmospheric boundary layer - Application for wind tunnels. Beuth Verlag, Berlin
[20] Mohamed, M.S., LaRue, J.C., 1990. The decay power law in grid generated turbulence. Journal of Fluid Mechanics 219, 195–214
[21] Burton T, Sharpe D, Jenkins N, Bossanyi E (2001) Wind Energy Handbook. John Wiley & Sons, Chichester